

# Miniature fiber Fabry-Perot sensors based on fusion splicing\*

ZHU Jia-li (朱佳利), WANG Ming (王鸣)\*\*, YANG Chun-di (杨春弟), and WANG Ting-ting (王婷婷)

*Jiangsu Key Lab. on Opto-Electronic Technology, School of Physical Science and Technology, Nanjing Normal University, Nanjing 210023, China*

(Received 25 December 2012)

©Tianjin University of Technology and Springer-Verlag Berlin Heidelberg 2013

Fiber-optic Fabry-Perot (F-P) sensors are widely investigated because they have several advantages over conventional sensors, such as immunity to electromagnetic interference, ability to operate under bad environments, high sensitivity and the potential for multiplexing. A new method to fabricate micro-cavity Fabry-Perot interferometer is introduced, which is fusion splicing a section of conventional single-mode fiber (SMF) and a section of hollow core or solid core photonic crystal fiber (PCF) together to form a micro-cavity at the splice joint. The technology of fusion splicing is discussed, and two miniature optical fiber sensors based on Fabry-Perot interference using fusion splicing are presented. The two sensors are completely made of fused silica, and have good high-temperature capability.

**Document code:** A **Article ID:** 1673-1905(2013)02-0085-4

**DOI** 10.1007/s11801-013-2432-9

Optical fiber fusion splicing is the process by which a permanent, low-loss, high-strength and welded joint is formed between two optical fibers<sup>[1]</sup>. It is known that when splicing together two micro-structured optical fibers (MOFs) or an MOF and a conventional optical fiber with the standard electric-arc method, the air-holes of the MOF can collapse completely in the vicinity of the splice<sup>[2,3]</sup>.

Usually, people choose appropriate splicing methods to avoid the collapsing. A novel method for low-loss splicing Ge-doped holey fibers with subwavelength core size and high numerical aperture fibers by using a conventional fusion splicer was demonstrated<sup>[4]</sup>. By introducing a relatively large overlap distance, splice loss of as low as 1 dB was achieved. A method for splicing a photonic crystal fiber (PCF) and a single-mode fiber (SMF) was proposed<sup>[5]</sup>, where nitrogen gas (N<sub>2</sub>) was pumped into the air holes of the PCF during fusion discharge to help reduce the splice loss. The air-hole collapse ratio of the PCF can be effectively avoided by adjusting the N<sub>2</sub> pressure. But sometimes, the collapsing of the microscopic air-holes was exploited to design useful devices. How to splice with a CO<sub>2</sub> laser to control the air-hole collapse was demonstrated<sup>[6]</sup>, which can give a considerably low loss for a solid-core PCF.

Fiber-optic Fabry-Perot interferometer (FPI) sensors have been intensively employed since the early 1980s for the detection of physical and chemical parameters, such as temperature, strain, gas phase concentrations and refractive index (RI), due to their simple configuration,

small size and high resolution<sup>[7-11]</sup>. Recently, a new method to fabricate FPI with micro-cavity was introduced by Villatoro<sup>[9]</sup> and Li<sup>[10]</sup>, respectively. It was fusion splicing a section of conventional SMF and a section of hollow core or solid core PCF together to form a micro-cavity at the splice joint.

In this paper, two miniature fiber Fabry-Perot (F-P) sensors are presented. The most important step in their production process is fusion splicing. One of them is made by splicing an SMF and a multi-mode fiber (MMF) (with core/cladding of 62.5 μm/125 μm) which is etched by hydrofluoric acid (HF) with no collapse. The other is fabricated by splicing an SMF and a PCF with the air holes collapsing completely. Both of them are made of silica fibers only. They are tested, and have good performance.

Fusion splicing is the most mature technology in splicing fibers, and commercial fusion splicers are widely used<sup>[12]</sup>. Fig.1 shows the current density or energy density distribution by contour lines<sup>[13]</sup>.

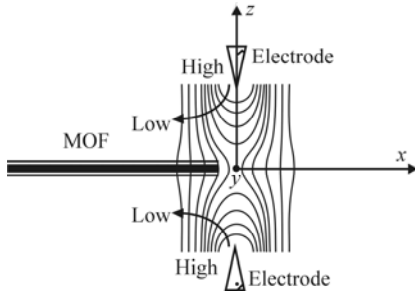
Optical fiber splice loss is caused by many factors including extrinsic ones and intrinsic ones. Extrinsic factors mainly include axis misalignment, axis tilt, end preparation and fiber physical deformation. Intrinsic factors mainly include optical fiber mode field mismatch, optical fiber core mismatch, fiber core section deformation and concentricity of core and cladding skewing. Among all the intrinsic factors, optical fiber mode field mismatch has the most impact, and loss  $\alpha_{\text{MFD}}$  caused by it is given by<sup>[12,14]</sup>

\* This work has been supported by the National Natural Science Foundation of China (Nos.91123015 and 61178044), and the Scientific Innovation Research of College Graduate in Jiangsu Province (No. CXLX11\_0890).

\*\* E-mail: wangming@njnu.edu.cn

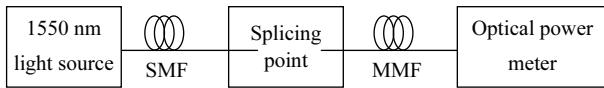
$$\alpha_{\text{MFD}} = -20 \log_{10} [2 / (\omega_1 / \omega_2 + \omega_2 / \omega_1)] \text{ (dB)}, \quad (1)$$

where  $\omega_1$  and  $\omega_2$  are the mode field diameters of input fiber and output fiber, respectively.



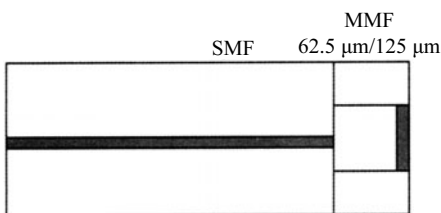
**Fig.1 Current density or energy density distribution by contour lines**

For the fusion splicing between an SMF and an MMF,  $\alpha_{\text{MFD}}$  is calculated as 11 dB. But by manual regulation of the splicing parameters as discharging current strength of 50 mA, premelting time of 170 ms and discharging time of 1000 ms, the loss can be reduced to 2.1 dB. Fig.2 shows the schematic diagram of experimental setup for testing splice loss. Therefore, choosing appropriate splicing parameters is very important during the splicing.



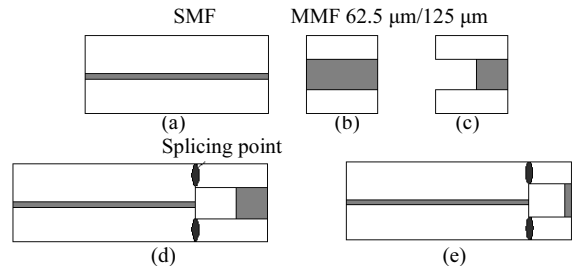
**Fig.2 Schematic diagram of experimental setup for testing splice loss**

Fig.3 shows the structure of a pressure sensor fabricated using fusion splicing. The left part is an SMF, and the right part is an MMF. A cavity is etched at one end of the MMF by HF. The other end of the MMF is lapped and used as a diaphragm. When the pressure applied to the sensor changes, the diaphragm deforms, which results in the cavity length changing. Since the length of F-P cavity can be demodulated, the loaded pressure can be obtained.



**Fig.3 Schematic diagram of the structure of the pressure sensor**

A schematic diagram of the production steps of the sensor is shown in Fig.4. An etched MMF needs to be spliced with an SMF, so the F-P cavity can be formed.



**Fig.4 Schematic diagram of fabrication steps of the sensor**

During the splicing, the current density distribution of the fusion splicer according to Fig.1 is given by<sup>[1]</sup>

$$i(r, z) = \frac{I_0}{2\pi\sigma^2(z)} \exp\left(-\frac{r^2}{2\sigma^2(z)}\right), \quad (2)$$

where  $\sigma(z) = \sigma_0(1 + Cz^2)^{-1/3}$  and  $r^2 = x^2 + y^2$ . We can see that the highest temperature appears on the top of the electrodes. On the axis of the electrodes, energy passes from the outer layer of the silica to the core. When the temperature is higher than 1670 °C, which is the softening point of the fiber, the surface tension can overcome the viscous force, so the cavity collapses. The collapse rate is given by<sup>[1]</sup>

$$V_{\text{collapse}} = \gamma / 2\eta, \quad (3)$$

where  $\gamma$  is the surface tension, and  $\eta$  is the viscous force. When using the automatic splicing program set by the commercial fusion splicer which is usually used for the splicing of two SMFs, the cavity can collapse, as shown in Fig.5.

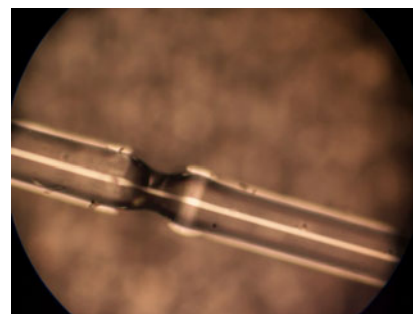


**Fig.5 Photo of collapsed cavity**

To avoid the cavity collapse, there should be some distance from the electrode to the MMF. The bigger the air cavity is, the longer the distance should be. Using the appropriate parameters, we can obtain an intact F-P cavity, as shown in Fig.6.

The performance of the pressure sensor is tested. Fig.7 shows the relation between pressure and cavity length of the sensor.

The fitting equation is  $L=49513.65-18.38P$ , and the

degree of fitting is 0.99925. The results show that when the pressure changes about 0.1 MPa, the cavity length  $L$  changes from 49513.63 nm to 49511.78 nm, reduced by 1.85 nm. The sensitivity of cavity length to pressure is 18.5 nm/MPa. It measures only 125  $\mu\text{m}$  in diameter.

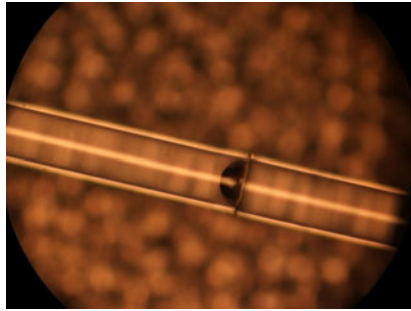


**Fig.6 Photo of the F-P cavity**

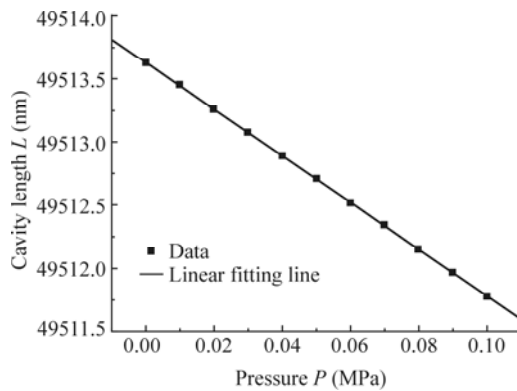


**Fig.7 Relation between pressure and cavity length**

Fig.8 shows the structure of a strain sensor. The left part is an SMF and the right part is a PCF. The PCF has a solid core diameter of 7.0  $\mu\text{m}$  and a mode field diameter of 3.9  $\mu\text{m}$  at 1550 nm. During the splicing, the air-holes of the PCF are intentionally collapsed in the vicinity of the splices. Some of the air is trapped, so an ellipsoidal air cavity is formed, which acts as the F-P cavity.

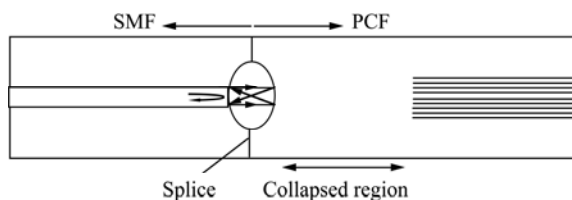


**Fig.8 Structure of the strain sensor**

To make sure there is enough reflection coupled into the SMF, we need to create a confocal cavity, which means the cavity length  $d$  needs to be approximately equal to the radius of curvature  $r$  of the two surfaces of the ellipsoidal cavity. The optimum splicing parameters

are shown in Tab.1.

**Tab.1 Optimum splicing parameters for creating a confocal cavity**

Parameter	Value
Premelting time	0.2 s
Premelting current strength	5 mA
Discharging current strength	7 mA
Discharging time	650 ms
Z-push distance	15 $\mu\text{m}$
Addition discharging current strength	7 mA
Addition discharging time	650 ms

After the first discharge, a small cavity is formed as shown in Fig.9(a). In this case,  $d$  is much smaller than  $r$ , and the two surfaces are rough. With increasing the time of discharge,  $d$  increases and  $r$  decreases. After the fourth discharge, we can obtain a confocal cavity with an intensity contrast of 30 dB, as shown in Fig.9(b). But if the discharge is carried out too many times, the internal pressure in the air cavity is isotropic, so the shape of the cavity changes no longer, and the intensity contrast decreases, as shown in Fig.9(c).

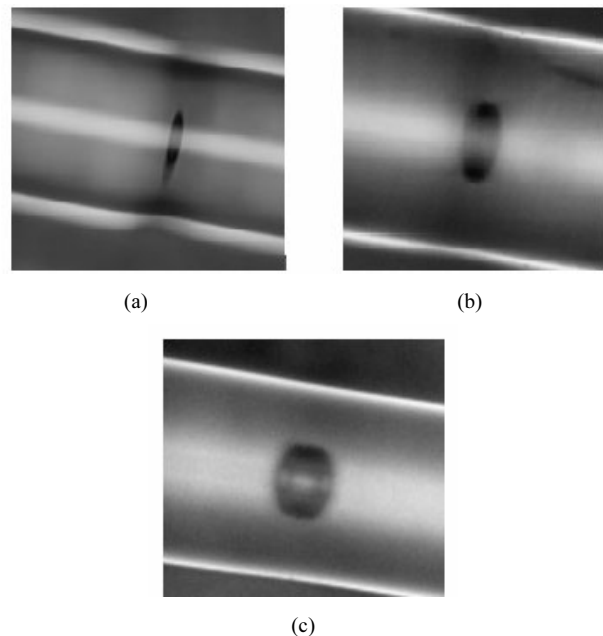


**Fig.9 Shapes of the cavity after (a) the first time, (b) the fourth time and (c) many times of discharge**

To test the performance of the sensor, we make two sensors, and apply axial stress on them and an FBG simultaneously. The sensor wavelength shift versus FBG wavelength shift at 25  $^{\circ}\text{C}$  is shown in Fig.10. The linear fitted slopes are 2.800 pm/pm for sensor1 and 2.704 pm/pm for sensor2, respectively.

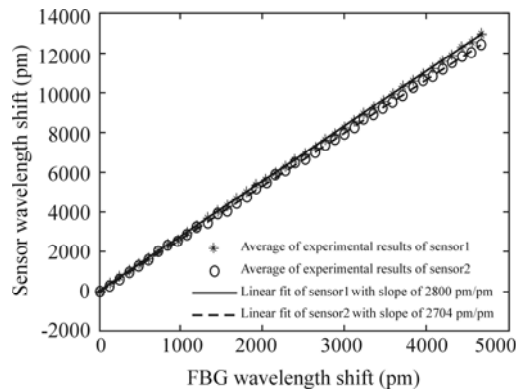


**Fig.10 Sensor wavelength shift versus FBG wavelength shift at 25 °C**

Fusion splicing is a very important technique in the fabrication of optical fiber sensors. We propose and demonstrate two novel miniature fiber-optic sensors which are fabricated directly on the tip of a fiber by fusion splicing. The splicing processes of these two sensors are specifically presented. Preliminary tests prove their potential for practical applications.

## References

- [1] A. D. Yablon, *Optical Fiber Fusion Splicing*, Heidelberg, Germany: Springer-Verlag Press, 1 (2005).
- [2] J. H. Chong, M. K. Rao, Y. Zhu and Y. P. Shum, *IEEE Photon. Technol. Lett.* **15**, 942 (2003).
- [3] J. Villatoro, V. P. Minkovich, V. Pruneri and G. Badenes, *Opt. Express* **15**, 1491 (2007).
- [4] M. L. V. Tse, H. Y. Tam, L. B. Fu, B. K. Thomas, L. Dong, C. Lu and P. K. A. Wai, *IEEE Photon. Technol. Lett.* **21**, 164 (2009).
- [5] Tao Zhu, Fufeng Xiao, Laicai Xu, Min Liu, Ming Deng and Kin Seng Chiang, *Opt. Express* **20**, 24465 (2009).
- [6] G. Fu, W. Jin, X. Fu and W. Bi, *IEEE Photon. Jour.* **4**, 1028 (2012).
- [7] Y. J. Rao, T. Zhu, X. C. Yang and D. W. Duan, *Opt. Lett.* **32**, 2662 (2007).
- [8] O. Frazao, S. H. Aref, J. M. Baptista, J. L. Santos, H. Latifi, F. Farahi, J. Kobelke and K. Schuster, *IEEE Photon. Technol. Lett.* **21**, 1229 (2009).
- [9] J. Villatoro, V. Finazzi, G. Coviello and V. Pruneri, *Opt. Lett.* **34**, 2441(2009).
- [10] Xu Ben, Li Jian-qing, Li Yi, Sun Miao, Zhao Xiao-wei and Dong Xin-yong, *Journal of Optoelectronics-Laser* **23**, 839 (2012). (in Chinese)
- [11] De-wen Duan, Yun-jiang Rao, Yu-song Hou and Tao Zhu, *Applied Optics* **51**, 1033 (2012).
- [12] Tang Chang-ping, Deng Ming, Zhu Tao and Bao Yun-jiang, *Journal of Optoelectronics-Laser* **22**, 1304 (2011). (in Chinese)
- [13] Limin Xiao, Wei Jin and M. S. Demokan, *Opt. Express* **13**, 9014 (2005).
- [14] Chong J. H. and Rao M. K., *Opt. Express* **11**, 1366 (2003).